

46. PLOTS OF CROSS SECTIONS AND RELATED QUANTITIES

(For neutrino plots, see review article "Neutrino Cross Section Measurements" by G.P. Zeller in this edition of RPP)

Jet Production in pp and $\bar{p}p$ Interactions

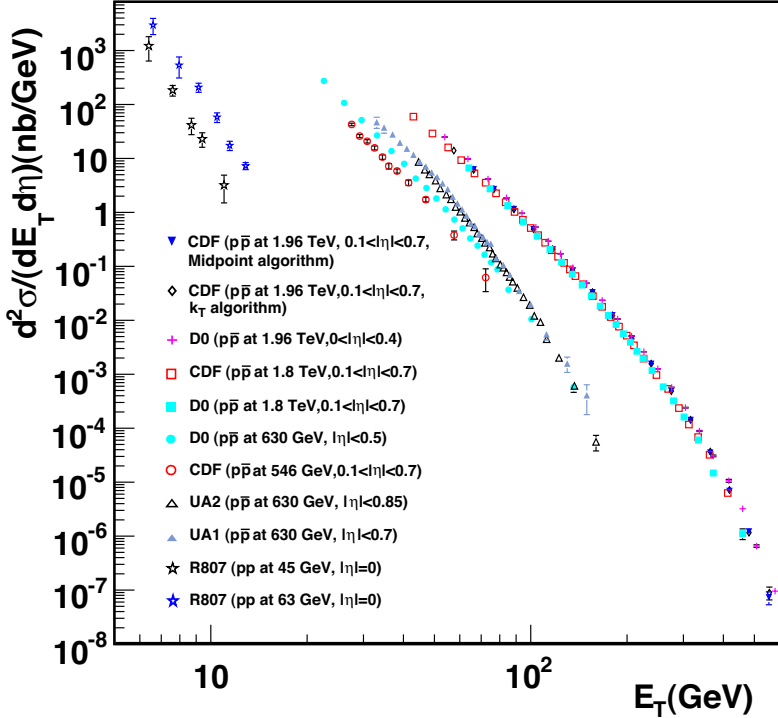


Figure 46.1: Inclusive differential jet cross sections plotted as a function of the jet transverse energy. The CDF and D0 measurements use a cone algorithm of radius 0.7 for all results shown except for the CDF measurements at 1.96 TeV which also use k_T with a D parameter of 0.7 and midpoint algorithms. The cone/ k_T results should be similar if $R_{cone} = D$. UA1 (UA2) uses a non-iterative cone algorithm with a radius of 1.0 (1.3). Recent NLO QCD predictions (such as CTEQ6M) provide a good description of the CDF and D0 jet cross sections, Rept. on Prog. in Phys. **70**, 89 (2007). Comparisons with the older cross sections are more difficult due to the nature of the jet algorithms used. **CDF**: Phys. Rev. **D75**, 092006 (2007), Phys. Rev. **D64**, 032001 (2001), Phys. Rev. Lett. **70**, 1376 (1993); **D0**: Phys. Rev. **D64**, 032003 (2001); **UA2**: Phys. Lett. **B257**, 232 (1991); **UA1**: Phys. Lett. **B172**, 461 (1986); **R807**: Phys. Lett. **B123**, 133 (1983). (Courtesy of J. Huston, Michigan State University, 2010.)

Direct γ Production in $\bar{p}p$ Interactions

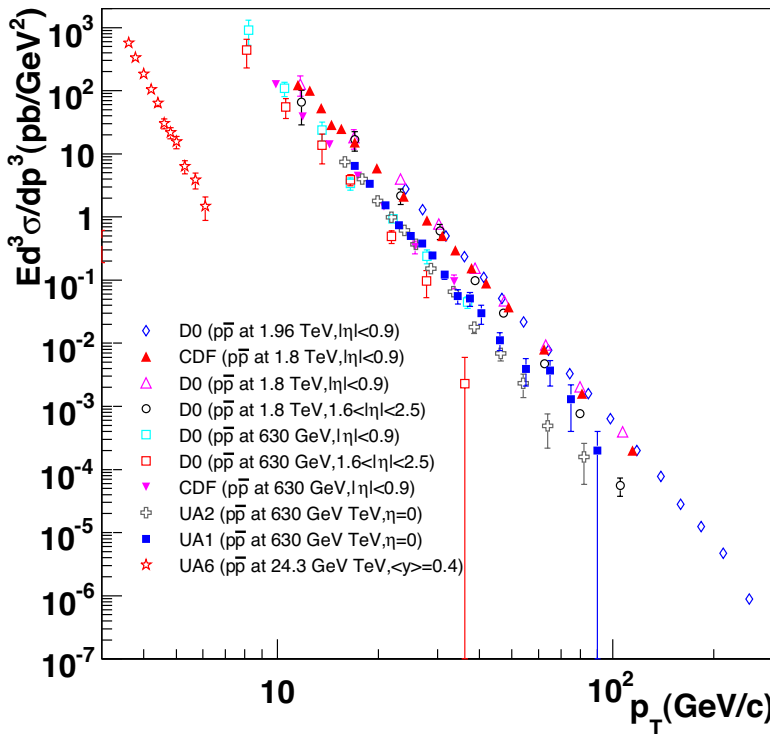


Figure 46.2: Isolated photon cross sections plotted as a function of the photon transverse momentum. The errors are either statistical only (CDF, D0 (1.96 TeV), UA1, UA2, UA6) or uncorrelated (D0 1.8 TeV, 630 GeV). The data are generally in good agreement with NLO QCD predictions, albeit with a tendency for the data to be above (below) the theory for lower (large) transverse momenta, Phys. Rev. **D59**, 074007 (1999). **D0**: Phys. Lett. **B639**, 151 (2006), Phys. Rev. Lett. **87**, 251805 (2001); **CDF**: Phys. Rev. **D65**, 112003 (2002); **UA6**: Phys. Lett. **B206**, 163 (1988); **UA1**: Phys. Lett. **B209**, 385 (1988); **UA2**: Phys. Lett. **B288**, 386 (1992). (Courtesy of J. Huston, Michigan State University, 2007.)

Differential Cross Section for W and Z Boson Production

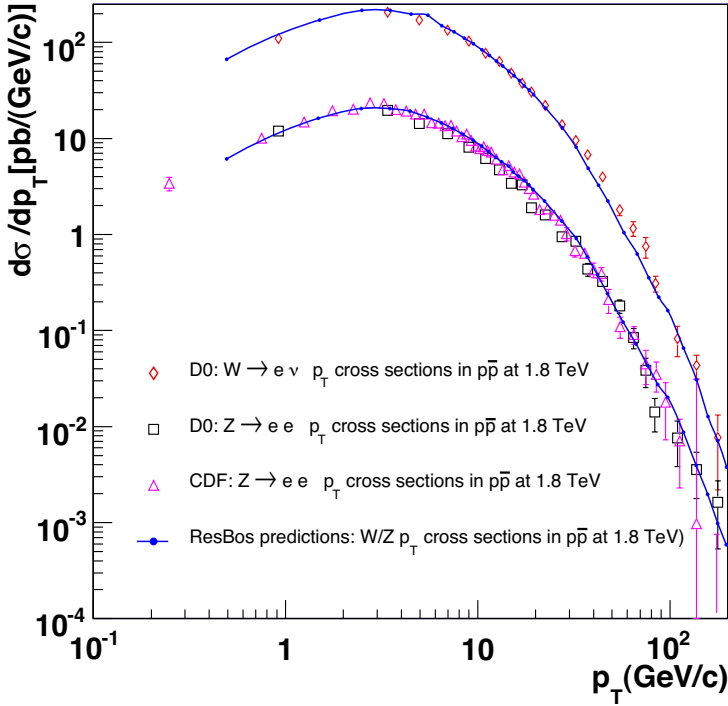


Figure 46.3: Differential cross sections for W and Z production shown as a function of the boson transverse momentum. The D0 results include only the statistical error while the CDF results include all errors except for the 3.9% integrated luminosity error. The results are in good agreement with theoretical predictions that include both the effects of NLO corrections and of q_T resummation, such as the ResBos (Phys. Rev. **D67**, 073016 (2003)) predictions indicated on the plot. **D0:** Phys. Lett. **B513**, 292 (2001), Phys. Rev. Lett. **84**, 2792 (2000). **CDF:** Phys. Rev. Lett. **84**, 845 (2000). (Courtesy of J. Huston, Michigan State University, 2007)

Pseudorapidity Distributions in $\bar{p}p$ Interactions

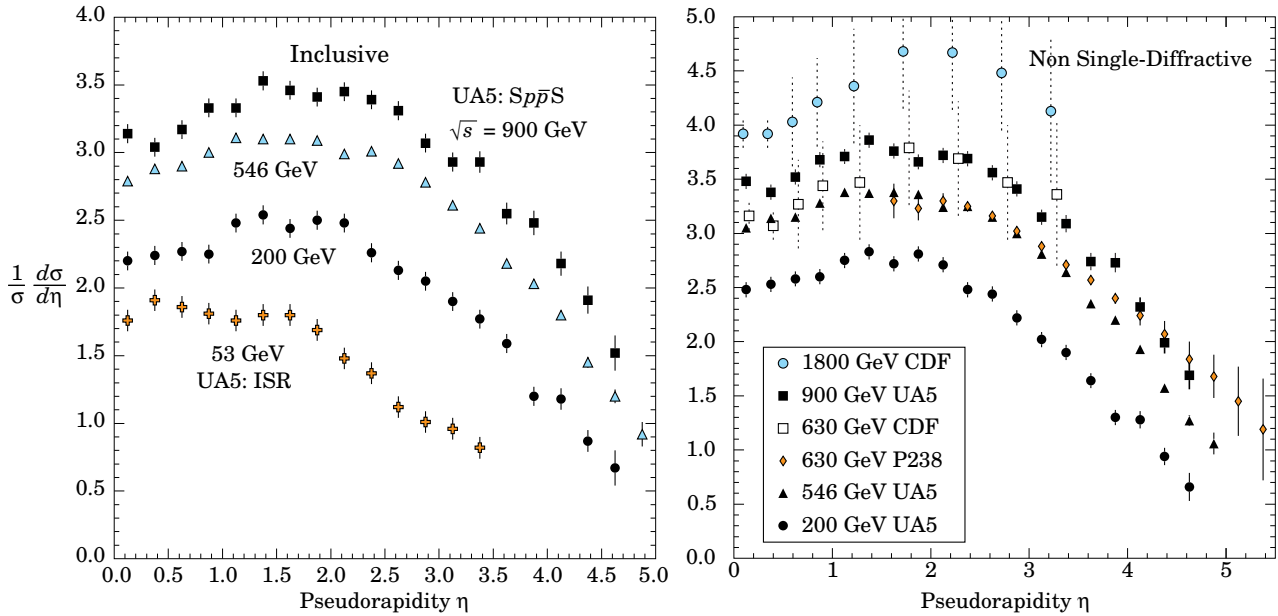


Figure 46.4: Charged particle pseudorapidity distributions in $p\bar{p}$ collisions for $53 \text{ GeV} \leq \sqrt{s} \leq 1800 \text{ GeV}$. UA5 data from the SppS are taken from G.J. Alner *et al.*, Z. Phys. **C33**, 1 (1986), and from the ISR from K. Alpgård *et al.*, Phys. Lett. **112B**, 193 (1982). The UA5 data are shown for both the full inelastic cross section and with singly diffractive events excluded. Additional non single-diffractive measurements are available from CDF at the Tevatron, F. Abe *et al.*, Phys. Rev. **D41**, 2330 (1990) and Experiment P238 at the SppS, R. Harr *et al.*, Phys. Lett. **B401**, 176 (1997). (Courtesy of D.R. Ward, Cambridge Univ., 1999)

Average Hadron Multiplicities in Hadronic e^+e^- Annihilation Events

Table 46.1: Average hadron multiplicities per hadronic e^+e^- annihilation event at $\sqrt{s} \approx 10, 29\text{--}35, 91$, and $130\text{--}200$ GeV. The rates given include decay products from resonances with $c\tau < 10$ cm, and include the corresponding anti-particle state. Correlations of the systematic uncertainties were considered for the calculation of the averages. (Updated May 2010 by O. Biebel, LMU, Munich)

Particle	$\sqrt{s} \approx 10$ GeV	$\sqrt{s} = 29\text{--}35$ GeV	$\sqrt{s} = 91$ GeV	$\sqrt{s} = 130\text{--}200$ GeV
Pseudoscalar mesons:				
π^+	6.6 ± 0.2	10.3 ± 0.4	17.02 ± 0.19	21.24 ± 0.39
π^0	3.2 ± 0.3	5.83 ± 0.28	9.42 ± 0.32	
K^+	0.90 ± 0.04	1.48 ± 0.09	2.228 ± 0.059	2.82 ± 0.19
K^0	0.91 ± 0.05	1.48 ± 0.07	2.049 ± 0.026	2.10 ± 0.12
η	0.20 ± 0.04	0.61 ± 0.07	1.049 ± 0.080	
$\eta(958)$	0.03 ± 0.01	0.26 ± 0.10	0.152 ± 0.020	
D^+	$0.194 \pm 0.019^{(a)}$	0.17 ± 0.03	0.175 ± 0.016	
D^0	$0.446 \pm 0.032^{(a)}$	0.45 ± 0.07	0.454 ± 0.030	
D_s^+	$0.063 \pm 0.014^{(a)}$	$0.45 \pm 0.20^{(b)}$	0.131 ± 0.021	
$B^{(c)}$	—	—	$0.165 \pm 0.026^{(d)}$	
B^+	—	—	$0.178 \pm 0.006^{(d)}$	
B_s^0	—	—	$0.057 \pm 0.013^{(d)}$	
Scalar mesons:				
$f_0(980)$	0.024 ± 0.006	$0.05 \pm 0.02^{(e)}$	0.146 ± 0.012	
$a_0(980)^\pm$	—	—	$0.27 \pm 0.11^{(f)}$	
Vector mesons:				
$\rho(770)^0$	0.35 ± 0.04	0.81 ± 0.08	1.231 ± 0.098	
$\rho(770)^\pm$	—	—	$2.40 \pm 0.43^{(f)}$	
$\omega(782)$	0.30 ± 0.08	—	1.016 ± 0.065	
$K^*(892)^+$	0.27 ± 0.03	0.64 ± 0.05	0.715 ± 0.059	
$K^*(892)^0$	0.29 ± 0.03	0.56 ± 0.06	0.738 ± 0.024	
$\phi(1020)$	0.044 ± 0.003	0.085 ± 0.011	0.0963 ± 0.0032	
$D^*(2010)^+$	$0.177 \pm 0.022^{(a)}$	0.43 ± 0.07	$0.1937 \pm 0.0057^{(g)}$	
$D^*(2007)^0$	$0.168 \pm 0.019^{(a)}$	0.27 ± 0.11	—	
$D_s^*(2112)^+$	$0.048 \pm 0.014^{(a)}$	—	$0.101 \pm 0.048^{(h)}$	
$B^*_{-}^{(i)}$	—	—	0.288 ± 0.026	
$J/\psi(1S)$	$0.00050 \pm 0.00005^{(a)}$	—	$0.0052 \pm 0.0004^{(j)}$	
$\psi(2S)$	—	—	$0.0023 \pm 0.0004^{(j)}$	
$\Upsilon(1S)$	—	—	$0.00014 \pm 0.00007^{(j)}$	
Pseudovector mesons:				
$f_1(1285)$	—	—	0.165 ± 0.051	
$f_1(1420)$	—	—	0.056 ± 0.012	
$\chi_{c1}(3510)$	—	—	$0.0041 \pm 0.0011^{(j)}$	
Tensor mesons:				
$f_2(1270)$	0.09 ± 0.02	0.14 ± 0.04	0.166 ± 0.020	
$f'_2(1525)$	—	—	0.012 ± 0.006	
$K_2^*(1430)^+$	—	0.09 ± 0.03	—	
$K_2^*(1430)^0$	—	0.12 ± 0.06	0.084 ± 0.022	
$B^{**}_{-}^{(k)}$	—	—	0.118 ± 0.024	
D_{s1}^{\pm}	—	—	$0.0052 \pm 0.0011^{(\ell)}$	
$D_{s2}^{*\pm}$	—	—	$0.0083 \pm 0.0031^{(\ell)}$	
Baryons:				
p	0.253 ± 0.016	0.640 ± 0.050	1.050 ± 0.032	1.41 ± 0.18
Λ	0.080 ± 0.007	0.205 ± 0.010	0.3915 ± 0.0065	0.39 ± 0.03
Σ^0	0.023 ± 0.008	—	0.076 ± 0.011	
Σ^-	—	—	0.081 ± 0.010	
Σ^+	—	—	0.107 ± 0.011	
Σ^{\pm}	—	—	0.174 ± 0.009	
Ξ^-	0.0059 ± 0.0007	0.0176 ± 0.0027	0.0258 ± 0.0010	
$\Delta(1232)^{++}$	0.040 ± 0.010	—	0.085 ± 0.014	
$\Sigma(1385)^-$	0.006 ± 0.002	0.017 ± 0.004	0.0240 ± 0.0017	
$\Sigma(1385)^+$	0.005 ± 0.001	0.017 ± 0.004	0.0239 ± 0.0015	
$\Sigma(1385)^{\pm}$	0.0106 ± 0.0020	0.033 ± 0.008	0.0462 ± 0.0028	
$\Xi(1530)^0$	0.0015 ± 0.0006	—	0.0068 ± 0.0006	
Ω^-	0.0007 ± 0.0004	0.014 ± 0.007	0.0016 ± 0.0003	
Λ_c^+	$0.074 \pm 0.031^{(m)}$	0.110 ± 0.050	0.078 ± 0.017	
Λ_b^0	—	—	0.031 ± 0.016	
$\Sigma_c^{++}, \Sigma_c^0$	0.014 ± 0.007	—	—	
$\Lambda(1520)$	0.008 ± 0.002	—	0.0222 ± 0.0027	

Notes for Table 46.1:

- (a) $\sigma_{\text{had}} = 3.33 \pm 0.05 \pm 0.21 \text{ nb}$ (**CLEO**: Phys. Rev. **D29**, 1254 (1984)) has been used in converting the measured cross sections to average hadron multiplicities.
- (b) $B(D_s \rightarrow \eta\pi, \eta'\pi)$ was used (RPP 1994).
- (c) Comprises both charged and neutral B meson states.
- (d) The Standard Model $B(Z \rightarrow b\bar{b}) = 0.217$ was used.
- (e) $x_p = p/p_{\text{beam}} > 0.1$ only.
- (f) Both charge states.
- (g) $B(D^*(2010)^+ \rightarrow D^0\pi^+) \times B(D^0 \rightarrow K^-\pi^+)$ has been used (RPP 2000).
- (h) $B(D_s^* \rightarrow D_S^+\gamma), B(D_s^+ \rightarrow \phi\pi^+), B(\phi \rightarrow K^+K^-)$ have been used (RPP 1998).
- (i) Any charge state (*i.e.*, B_d^* , B_u^* , or B_s^*).
- (j) $B(Z \rightarrow \text{hadrons}) = 0.699$ was used (RPP 1994).
- (k) Any charge state (*i.e.*, B_d^{**} , B_u^{**} , or B_s^{**}).
- (l) Assumes $B(D_{s1}^+ \rightarrow D^{*+}K^0 + D^{*0}K^+) = 100\%$ and $B(D_{s2}^+ \rightarrow D^0K^+) = 45\%$.
- (m) The value was derived from the cross section of $\Lambda_c^+ \rightarrow p\pi K$ using (a) and assuming the branching fraction to be $(5.0 \pm 1.3)\%$ (RPP 2004).

References for Table 46.1:

- RPP 1992:** Phys. Rev. **D45** (1992) and references therein.
- RPP 1994:** Phys. Rev. **D50**, 1173 (1994) and references therein.
- RPP 1996:** Phys. Rev. **D54**, 1 (1996) and references therein.
- RPP 1998:** Eur. Phys. J. **C3**, 1 (1998) and references therein.
- RPP 2000:** Eur. Phys. J. **C15**, 1 (2000) and references therein.
- RPP 2002:** Phys. Rev. **D66**, 010001 (2002) and references therein.
- RPP 2004:** Phys. Lett. **B592**, 1 (2004) and references therein.
- RPP 2006:** J. Phys. **G33**, 1 (2006) and references therein.
- RPP 2008:** Phys. Lett. **B667**, 1 (2008) and references therein.
- R. Marshall, Rept. on Prog. in Phys. **52**, 1329 (1989). A. De Angelis, J. Phys. **G19**, 1233 (1993) and references therein.
- ALEPH:** D. Buskulic *et al.*: Phys. Lett. **B295**, 396 (1992); Z. Phys. **C64**, 361 (1994); **C69**, 15 (1996); **C69**, 379 (1996); **C73**, 409 (1997); and R. Barate *et al.*: Z. Phys. **C74**, 451 (1997); Phys. Reports **294**, 1 (1998); Eur. Phys. J. **C5**, 205 (1998); **C16**, 597 (2000); **C16**, 613 (2000); and A. Heister *et al.*: Phys. Lett. **B526**, 34 (2002); **B528**, 19 (2002).
- ARGUS:** H. Albrecht *et al.*: Phys. Lett. **230B**, 169 (1989); Z. Phys. **C44**, 547 (1989); **C46**, 15 (1990); **C54**, 1 (1992); **C58**, 199 (1993); **C61**, 1 (1994); Phys. Rep. **276**, 223 (1996).
- BaBar:** B. Aubert *et al.*: Phys. Rev. Lett. **87**, 162002 (2001); Phys. Rev. **D65**, 091104 (2002).
- Belle:** K. Abe *et al.*, Phys. Rev. Lett. **88**, 052001 (2002); and R. Seuster *et al.*, Phys. Rev. **D73**, 032002 (2006).
- CELLO:** H.J. Behrend *et al.*: Z. Phys. **C46**, 397 (1990); **C47**, 1 (1990).
- CLEO:** D. Bortoletto *et al.*, Phys. Rev. **D37**, 1719 (1988); erratum *ibid.* **D39**, 1471 (1989); and M. Artuso *et al.*, Phys. Rev. **D70**, 112001 (2004).
- Crystal Ball:** Ch. Bieler *et al.*, Z. Phys. **C49**, 225 (1991).
- DELPHI:** P. Abreu *et al.*: Z. Phys. **C57**, 181 (1993); **C59**, 533 (1993); **C61**, 407 (1994); **C65**, 587 (1995); **C67**, 543 (1995); **C68**, 353 (1995); **C73**, 61 (1996); Nucl. Phys. **B444**, 3 (1995); Phys. Lett. **B341**, 109 (1994); **B345**, 598 (1995); **B361**, 207 (1995); **B372**, 172 (1996); **B379**, 309 (1996); **B416**, 233 (1998); **B449**, 364 (1999); **B475**, 429 (2000); Eur. Phys. J. **C6**, 19 (1999); **C5**, 585 (1998); **C18**, 203 (2000); and J. Abdallah *et al.*, Phys. Lett. **B569**, 129 (2003); Phys. Lett. **B576**, 29 (2003); Eur. Phys. J. **C44**, 299 (2005); and W. Adam *et al.*: Z. Phys. **C69**, 561 (1996); **C70**, 371 (1996).
- HRS:** S. Abachi *et al.*, Phys. Rev. Lett. **57**, 1990 (1986); and M. Derrick *et al.*, Phys. Rev. **D35**, 2639 (1987).
- L3:** M. Acciarri *et al.*: Phys. Lett. **B328**, 223 (1994); **B345**, 589 (1995); **B371**, 126 (1996); **B371**, 137 (1996); **B393**, 465 (1997); **B404**, 390 (1997); **B407**, 351 (1997); **B407**, 389 (1997), erratum *ibid.* **B427**, 409 (1998); **B453**, 94 (1999); **B479**, 79 (2000).
- MARK II:** H. Schellman *et al.*, Phys. Rev. **D31**, 3013 (1985); and G. Wormser *et al.*, Phys. Rev. Lett. **61**, 1057 (1988).
- JADE:** W. Bartel *et al.*, Z. Phys. **C20**, 187 (1983); and D.D. Pietzl *et al.*, Z. Phys. **C46**, 1 (1990).
- OPAL:** R. Akers *et al.*: Z. Phys. **C63**, 181 (1994); **C66**, 555 (1995); **C67**, 389 (1995); **C68**, 1 (1995); and G. Alexander *et al.*: Phys. Lett. **B358**, 162 (1995); Z. Phys. **C70**, 197 (1996); **C72**, 1 (1996); **C72**, 191 (1996); **C73**, 569 (1997); **C73**, 587 (1997); Phys. Lett. **B370**, 185 (1996); and K. Ackerstaff *et al.*: Z. Phys. **C75**, 192 (1997); Phys. Lett. **B412**, 210 (1997); Eur. Phys. J. **C1**, 439 (1998); **C4**, 19 (1998); **C5**, 1 (1998); **C5**, 411 (1998); and G. Abbiendi *et al.*: Eur. Phys. J. **C16**, 185 (2000); **C17**, 373 (2000).
- PLUTO:** Ch. Berger *et al.*, Phys. Lett. **104B**, 79 (1981).
- SLD:** K. Abe, Phys. Rev. **D59**, 052001 (1999); Phys. Rev. **D69**, 072003 (2004).
- TASSO:** H. Aihara *et al.*, Z. Phys. **C27**, 27 (1985).
- TPC:** H. Aihara *et al.*, Phys. Rev. Lett. **53**, 2378 (1984).

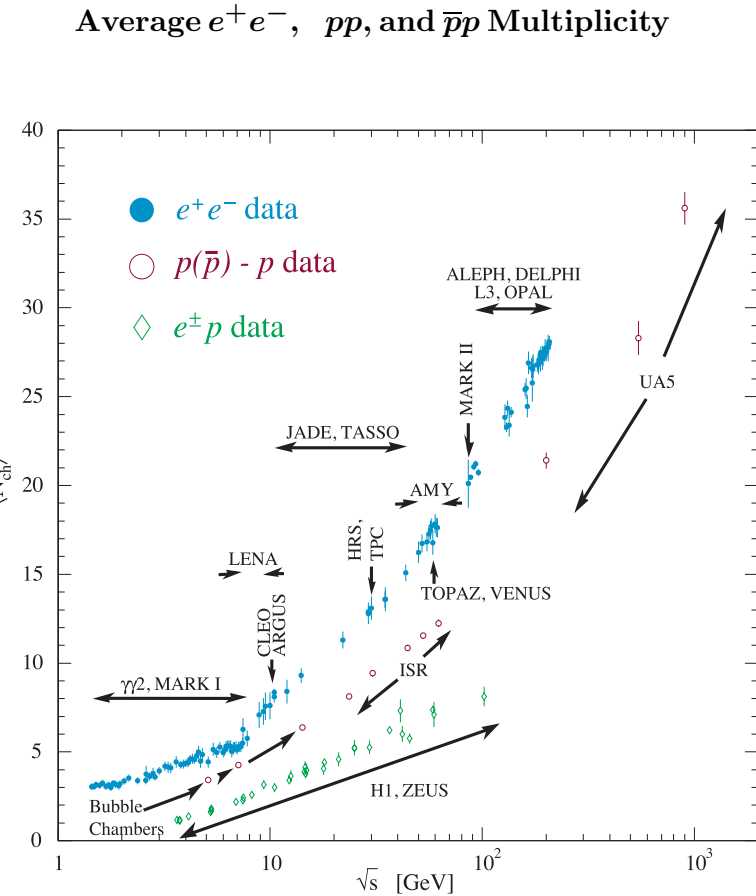


Figure 46.5: Average multiplicity as a function of \sqrt{s} for e^+e^- and $p\bar{p}$ annihilations, and pp and ep collisions. The indicated errors are statistical and systematic errors added in quadrature, except when no systematic errors are given. Files of the data shown in this figure are given in <http://pdg.lbl.gov/current/avg-multiplicity/>.

e^+e^- : Most e^+e^- measurements include contributions from K_S^0 and Λ decays. The $\gamma\gamma 2$ and MARK I measurements contain a systematic 5% error. Points at identical energies have been spread horizontally for clarity:

ALEPH: D. Buskulic *et al.*, Z. Phys. **C69**, 15 (1995); and Z. Phys. **C73**, 409 (1997);
A. Heister *et al.*, Eur. Phys. J. **C35**, 457 (2004).

ARGUS: H. Albrecht *et al.*, Z. Phys. **C54**, 13 (1992).

DELPHI: P. Abreu *et al.*, Eur. Phys. J. **C6**, 19 (1999); Phys. Lett. **B372**, 172 (1996); Phys. Lett. **B416**, 233 (1998); and Eur. Phys. J. **C18**, 203 (2000).

L3: M. Acciarri *et al.*, Phys. Lett. **B371**, 137 (1996); Phys. Lett. **B404**, 390 (1997); and Phys. Lett. **B444**, 569 (1998);
P. Achard *et al.*, Phys. Reports **339**, 71 (2004).

OPAL: G. Abbiendi *et al.*, Eur. Phys. J. **C16**, 185 (2000); and Eur. Phys. J. **C37**, 25 (2004);
K. Ackerstaff *et al.*, Z. Phys. **C75**, 193 (1997);
P.D. Acton *et al.*, Z. Phys. **C53**, 539 (1992) and references therein;
R. Akers *et al.*, Z. Phys. **C68**, 203 (1995).

TOPAZ: K. Nakabayashi *et al.*, Phys. Lett. **B413**, 447 (1997).

VENUS: K. Okabe *et al.*, Phys. Lett. **B423**, 407 (1998).

$e^\pm p$: Multiplicities have been measured in the current fragmentation region of the Breit frame:

H1: C. Adloff *et al.*, Nucl. Phys. **B504**, 3 (1997); F.D. Aaron *et al.*, Phys. Lett. **B654**, 148 (2007).

ZEUS: J. Breitweg *et al.*, Eur. Phys. J. **C11**, 251 (1999);
S. Chekanov *et al.*, Phys. Lett. **B510**, 36 (2001).

$p(\bar{p})$: The errors of the $p(\bar{p})$ measurements are the quadratically added statistical and systematic errors, except for the bubble chamber measurements for which only statistical errors are given in the references. The values measured by UA5 exclude single diffractive dissociation:

bubble chamber: J. Benecke *et al.*, Nucl. Phys. **B76**, 29 (1976); W.M. Morse *et al.*, Phys. Rev. **D15**, 66 (1977).

ISR: A. Breakstone *et al.*, Phys. Rev. **D30**, 528 (1984).

UA5: G.J. Alner *et al.*, Phys. Lett. **167B**, 476 (1986);
R.E. Ansorge *et al.*, Z. Phys. **C43**, 357 (1989).

(Courtesy of O. Biebel, LMU, Munich, 2010)

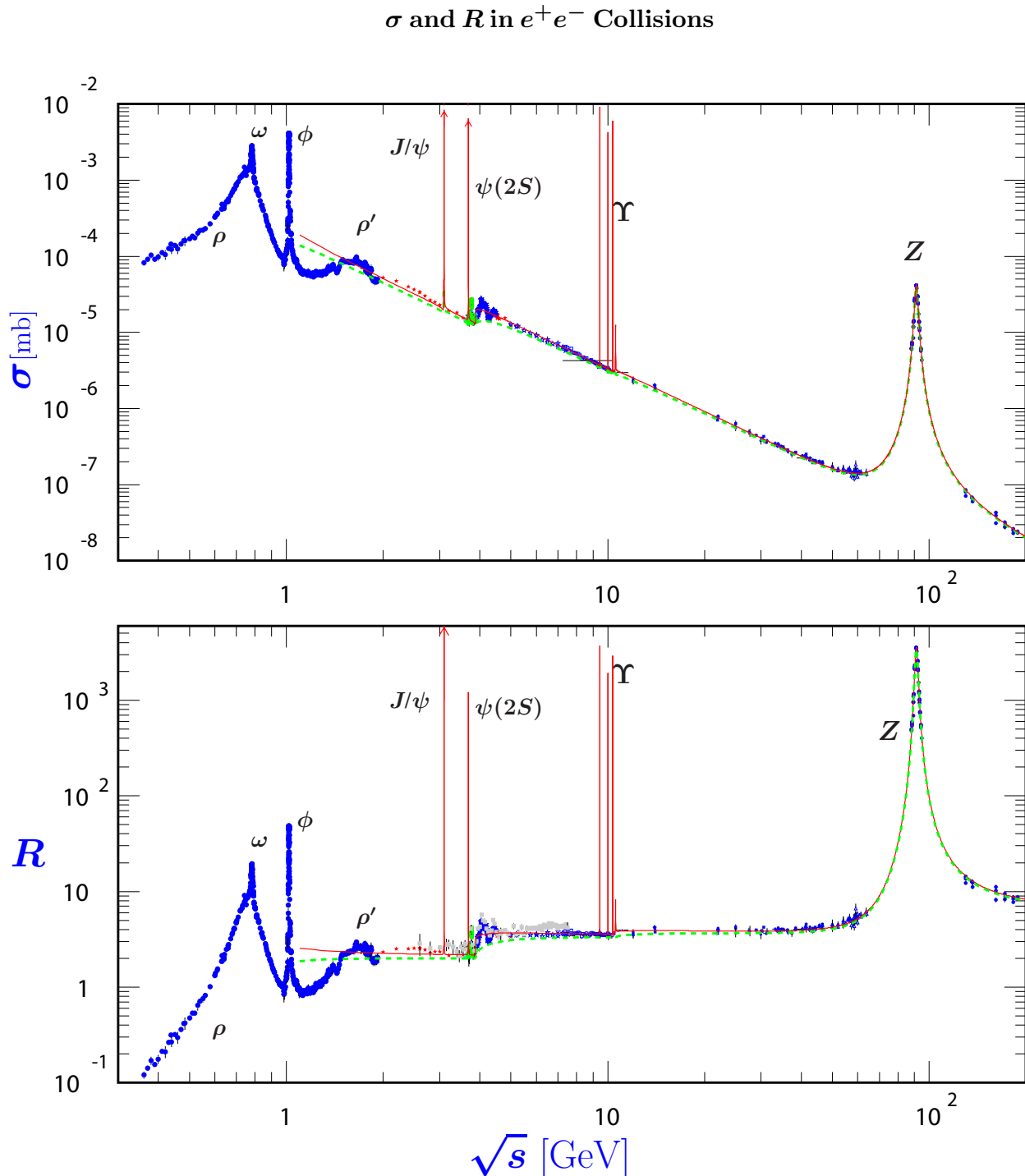


Figure 46.6: World data on the total cross section of $e^+e^- \rightarrow \text{hadrons}$ and the ratio $R(s) = \sigma(e^+e^- \rightarrow \text{hadrons}, s)/\sigma(e^+e^- \rightarrow \mu^+\mu^-, s)$. $\sigma(e^+e^- \rightarrow \text{hadrons}, s)$ is the experimental cross section corrected for initial state radiation and electron-positron vertex loops, $\sigma(e^+e^- \rightarrow \mu^+\mu^-, s) = 4\pi\alpha^2(s)/3s$. Data errors are total below 2 GeV and statistical above 2 GeV. The curves are an educative guide: the broken one (green) is a naive quark-parton model prediction, and the solid one (red) is 3-loop pQCD prediction (see “Quantum Chromodynamics” section of this Review, Eq. (9.7) or, for more details, K. G. Chetyrkin *et al.*, Nucl. Phys. **B586**, 56 (2000) (Erratum *ibid.* **B634**, 413 (2002)). Breit-Wigner parameterizations of J/ψ , $\psi(2S)$, and $\Upsilon(nS)$, $n = 1, 2, 3, 4$ are also shown. The full list of references to the original data and the details of the R ratio extraction from them can be found in [[arXiv:hep-ph/0312114](#)]. Corresponding computer-readable data files are available at <http://pdg.lbl.gov/current/xsect/>. (Courtesy of the COMPAS (Protvino) and HEPDATA (Durham) Groups, May 2010.)

R in Light-Flavor, Charm, and Beauty Threshold Regions

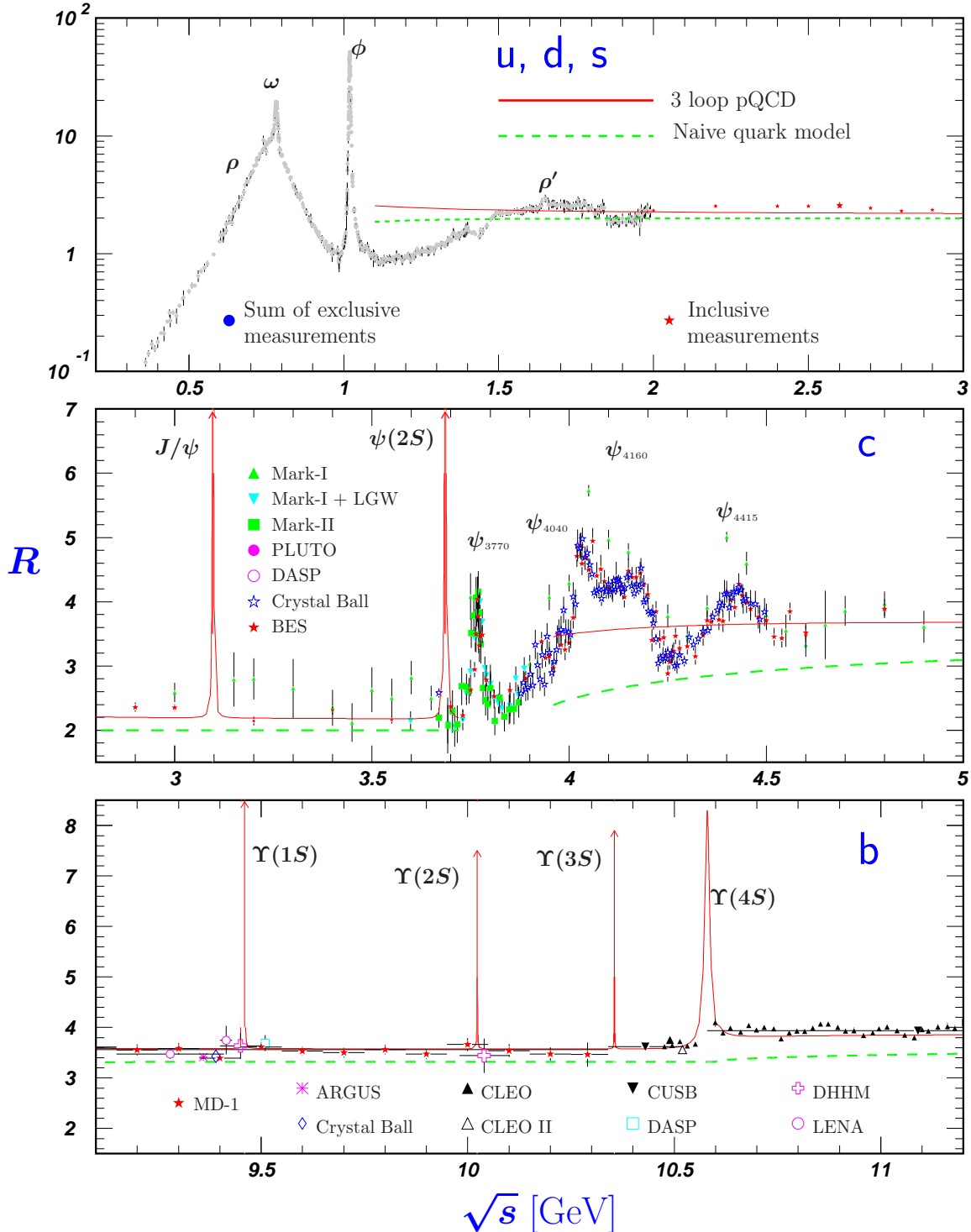


Figure 46.7: R in the light-flavor, charm, and beauty threshold regions. Data errors are total below 2 GeV and statistical above 2 GeV. The curves are the same as in Fig. 46.6. **Note:** CLEO data above $\Upsilon(4S)$ were not fully corrected for radiative effects, and we retain them on the plot only for illustrative purposes with a normalization factor of 0.8. The full list of references to the original data and the details of the R ratio extraction from them can be found in [arXiv:hep-ph/0312114]. The computer-readable data are available at <http://pdg.lbl.gov/current/xsect/>. (Courtesy of the COMPAS (Protvino) and HEPDATA (Durham) Groups, May 2010.)

Annihilation Cross Section Near M_Z

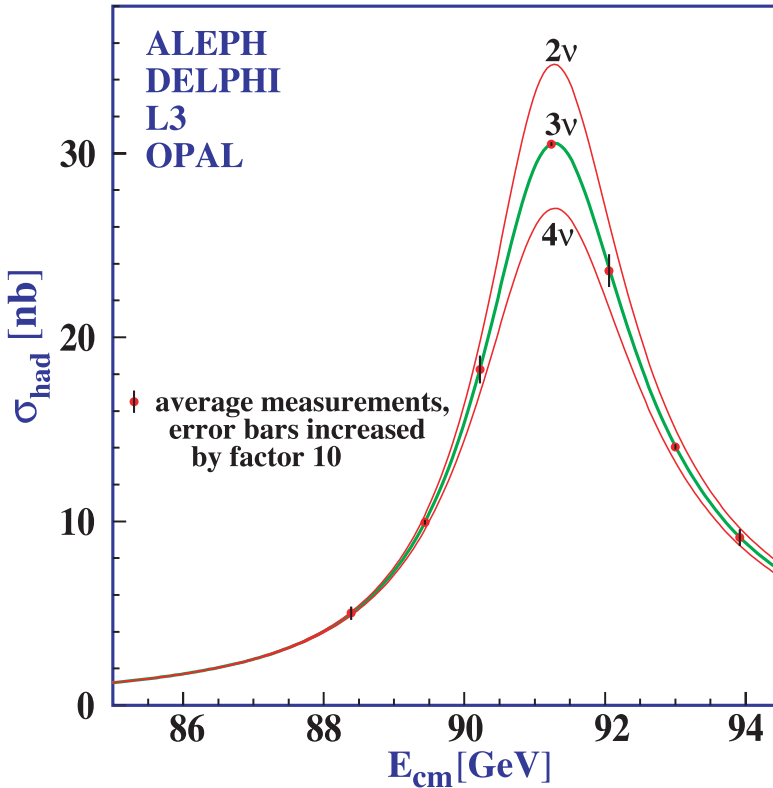


Figure 46.8: Combined data from the ALEPH, DELPHI, L3, and OPAL Collaborations for the cross section in e^+e^- annihilation into hadronic final states as a function of the center-of-mass energy near the Z pole. The curves show the predictions of the Standard Model with two, three, and four species of light neutrinos. The asymmetry of the curve is produced by initial-state radiation. Note that the error bars have been increased by a factor ten for display purposes. References:

ALEPH: R. Barate *et al.*, Eur. Phys. J. **C14**, 1 (2000).

DELPHI: P. Abreu *et al.*, Eur. Phys. J. **C16**, 371 (2000).

L3: M. Acciarri *et al.*, Eur. Phys. J. **C16**, 1 (2000).

OPAL: G. Abbiendi *et al.*, Eur. Phys. J. **C19**, 587 (2001).

Combination: The ALEPH, DELPHI, L3, OPAL, SLD Collaborations, the LEP Electroweak Working Group, and the SLD Electroweak and Heavy Flavor Groups, Phys. Rept. **427**, 257 (2006) [[arXiv:hep-ex/0509008](https://arxiv.org/abs/hep-ex/0509008)].

(Courtesy of M. Grünewald and the LEP Electroweak Working Group, 2007)

Table 46.2: Total hadronic cross section. Analytic S -matrix and Regge theory suggest a variety of parameterizations of total cross sections at high energies with different areas of applicability and fits quality.

A ranking procedure, based on measures of different aspects of the quality of the fits to the current evaluated experimental database, allows one to single out the following parameterization of highest rank [1]

$$\sigma^{ab} = Z^{ab} + B^{ab} \log^2(s/s_M) + Y_1^{ab}(s_M/s)^{\eta_1} - Y_2^{ab}(s_M/s)^{\eta_2} \quad \sigma^{\overline{ab}} = Z^{ab} + B^{ab} \log^2(s/s_M) + Y_1^{ab}(s_M/s)^{\eta_1} + Y_2^{ab}(s_M/s)^{\eta_2},$$

where Z^{ab} , $B^{a(p,n,\gamma*)} = \pi \frac{(hc)^2}{M^2}$, $B^{ad} = \lambda \pi \frac{(hc)^2}{M^2}$ (dimensionless factor λ introduced to test the universality for nuclei targets), Y_i^{ab} are in mb; s , $s_M = (m_a + m_b + M)^2$ are in GeV^2 ; m_a , m_b , $[m_{\gamma^*} = m_{\rho(770)}]$ are the masses of initial state particles, and M – the mass parameter defining the rate of universal rise of the cross sections are all in GeV . Parameters M , η_1 and η_2 are universal for all collisions considered. Terms $Z^{ab} + B^{ab} \log^2(s/s_M)$ represent the pomerons. The exponents η_1 and η_2 represent lower-lying C-even and C-odd exchanges, respectively. In addition to total cross sections σ , the measured ratios of the real-to-imaginary parts of the forward scattering amplitudes $\rho = \text{Re}(T)/\text{Im}(T)$ are included in the fits by using s to u crossing symmetry and differential dispersion relations.

Exact factorization hypothesis was used for both Z^{ab} and $B^{ab} \log^2(s/s_M)$ to extend the universal rise of the total hadronic cross sections to the $\gamma p \rightarrow \text{hadrons}$ and $\gamma\gamma \rightarrow \text{hadrons}$ collisions. This results in substitutions: $Z^{\gamma p} + \pi \frac{(hc)^2}{M^2} \log^2(s/s_M) \Rightarrow \delta [Z^{pp} + \pi \frac{(hc)^2}{M^2} \log^2(s/s_M)]$, and $Z^{\gamma\gamma} + \pi \frac{(hc)^2}{M^2} \log^2(s/s_M) \Rightarrow \delta^2 [Z^{pp} + \pi \frac{(hc)^2}{M^2} \log^2(s/s_M)]$, with the additional parameter δ . Simultaneous fit was made to the 2011-updated data for all collisions listed in the central column of the table. The total number of adjusted parameters is 34. Asymptotic parameters (Z , M , λ , δ , η_1 , η_2) thus obtained were then fixed and used as inputs to fits by groups to check a stability of the whole situation with description of the high energy data. Results are shown in the right hand part of the table. All fits included data above $\sqrt{s_{\min}} = 5 \text{ GeV}$ with overall $\chi^2/\text{dof} = 0.96$.

M=2.15(2), $\eta_1=0.462(2)$, $\eta_2=0.550(5)$			Beam/ Target	$\delta=0.003056(15)$, $\lambda=1.630(35)$			χ^2/dof by groups
Z	Y_1	Y_2		Z	Y_1	Y_2	
34.71(15)	12.72(19)	7.35(8)	$\bar{p}(p)/p$	34.71(15)	12.72(6)	7.35(7)	
35.00(18)	12.19(34)	6.62(16)	$\bar{p}(p)n$	35.00(16)	12.19(45)	6.6(2)	1.051
34.9(1.4)	-55(23)	-57(24)	Σ^-/p	34.9(1.4)	-55(6)	-57(8)	0.558
19.02(13)	9.22(16)	1.75(3)	π^\pm/p	19.02(13)	9.22(3)	1.75(3)	1.020
16.55(9)	4.02(14)	3.39(4)	K^\pm/p	16.55(9)	4.02(3)	3.39(3)	
16.49(10)	3.44(19)	1.82(7)	K^\pm/n	16.49(6)	3.44(16)	1.82(7)	0.737
0.0128(12)		γ/p	0.00128(4)				
-0.034(0.183)·10 ⁻⁴		γ/γ	-0.034(166)·10 ⁻⁴				0.722
65.02(38)	29.04(44)	14.9(2)	$\bar{p}(p)/d$	65.02(16)	29.04(39)	14.9(2)	1.524
37.06(30)	18.28(41)	0.34(9)	π^\pm/d	37.06(7)	18.28(19)	0.34(9)	0.747
32.34(22)	7.33(34)	5.59(9)	K^\pm/d	32.34(6)	7.33(16)	5.59(7)	0.819

The fitted functions are shown in the following figures, along with one-standard-deviation error bands. Whenever the reduced χ^2 is greater than one, a scale factor has been included to evaluate the parameter values and to draw the error bands. Where appropriate, statistical and systematic errors were combined quadratically in constructing weights for all fits. Only statistical error bars are shown on the plots. Vertical arrows indicate lower limits on the p_{lab} or \sqrt{s} range used in the fits. Database used in the fits now includes pp data from TOTEM experiment [2] and new data in the RHIC energy range from ARGO-YBJ cosmic ray experiment [3]. The modifications of the universal asymptotic term are motivated by ideas, suggestions and results from the old and recent papers [4-14]. Computer-readable data files are available at <http://pdg.lbl.gov/current/xsect/>. (Courtesy of the COMPAS group, IHEP, Protvino, April 2012)

References:

1. J.R. Cudell *et al.* (COMPETE Collab.), Phys. Rev. **D65**, 074024 (2002).
2. G. Antchev *et al.* (TOTEM Collaboration), Europhys. Lett. **96**, 21002 (2011).
3. G. Aielli *et al.* (ARGO-YBJ Collaboration), Phys. Rev. **D80**, 092004 (2009).
4. K. Igi and M. Ishida, Phys. Rev. **D66**, 034023 (2002), Phys. Lett. **B622**, 286 (2005).
5. M. M. Block and F. Halzen, Phys. Rev. **D70**, 091901 (2004), Phys. Rev. **D72**, 036006 (2005).
6. M. Ishida and K. Igi, Prog. Theor. Phys. Suppl. **187**, 297 (2011).
7. M. Ishida and V. Barger, Phys. Rev. D **84**, 014027 (2011).
8. F. Halzen, K. Igi, M. Ishida and C. S. Kim, Phys. Rev. **D85**, 074020 (2012).
9. S. S. Gershtein, A. A. Logunov, Sov. J. Nucl. Phys. **39**, 960 (1984) [Yad. Fiz. **39**, 1514 (1984)].
10. E. Iancu and R. Venugopalan, In Hwa, R.C. (ed.) *et al.: Quark gluon plasma 249-3363* [[hep-ph/0303204](https://arxiv.org/abs/hep-ph/0303204)].
11. L. Frankfurt, M. Strikman, and M. Zhalov, Phys. Lett. **B616**, 59 (2005).
12. Y. I. Azimov, Phys. Rev. **D84**, 056012 (2011).
13. D. A. Fagundes, M. J. Menon, Nucl. Phys. **A880**, 1 (2012),
14. D. A. Fagundes, M. J. Menon, and P. V. R. G. Silva, Braz. J. Phys. **42**, 452 (2012) [[arXiv:1112.4704](https://arxiv.org/abs/1112.4704)].

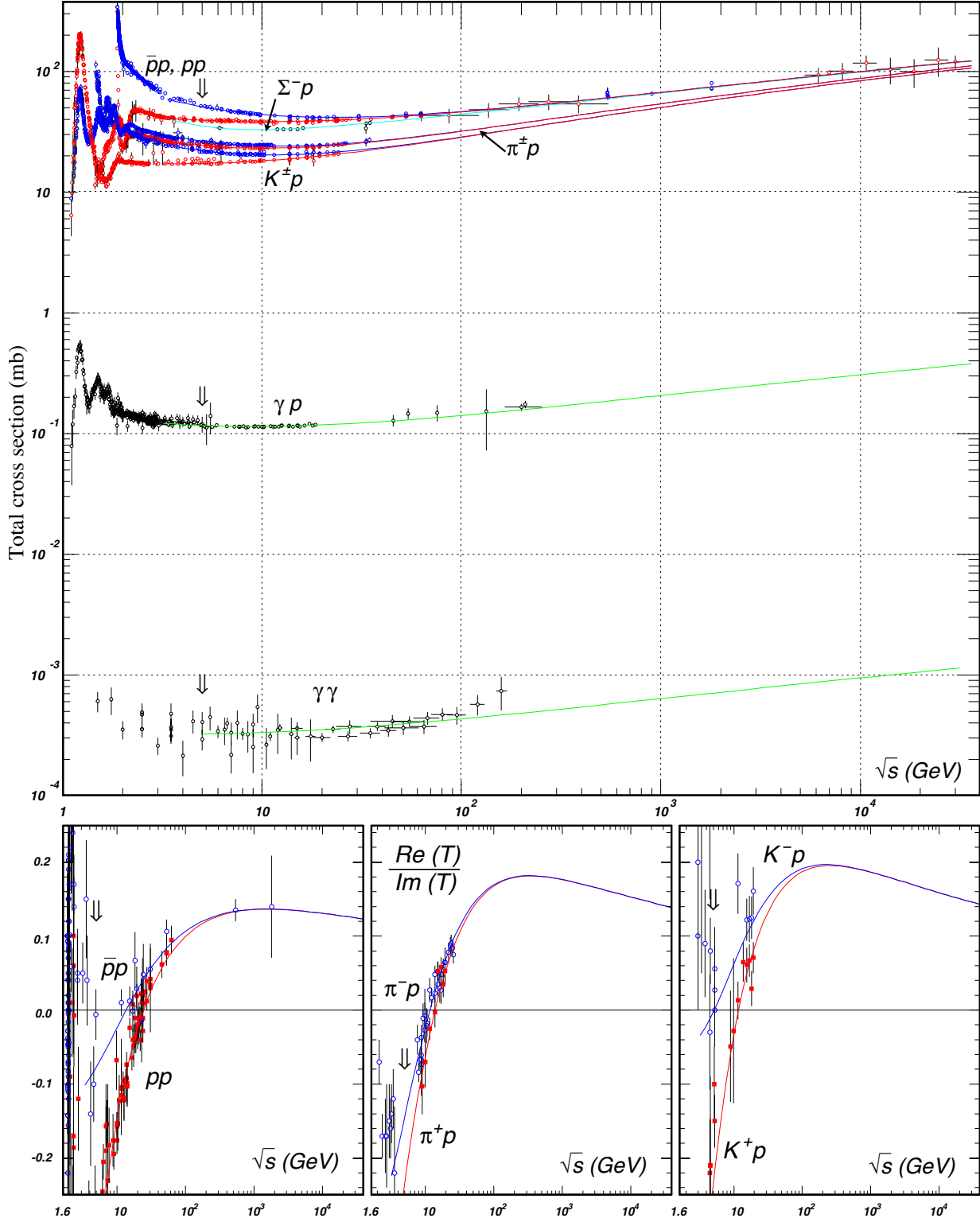


Figure 46.9: Summary of hadronic, γp , and $\gamma\gamma$ total cross sections, and ratio of the real to imaginary parts of the forward hadronic amplitudes. Corresponding computer-readable data files may be found at <http://pdg.lbl.gov/current/xsect/>. (Courtesy of the COMPAS group, IHEP, Protvino, April 2012.)

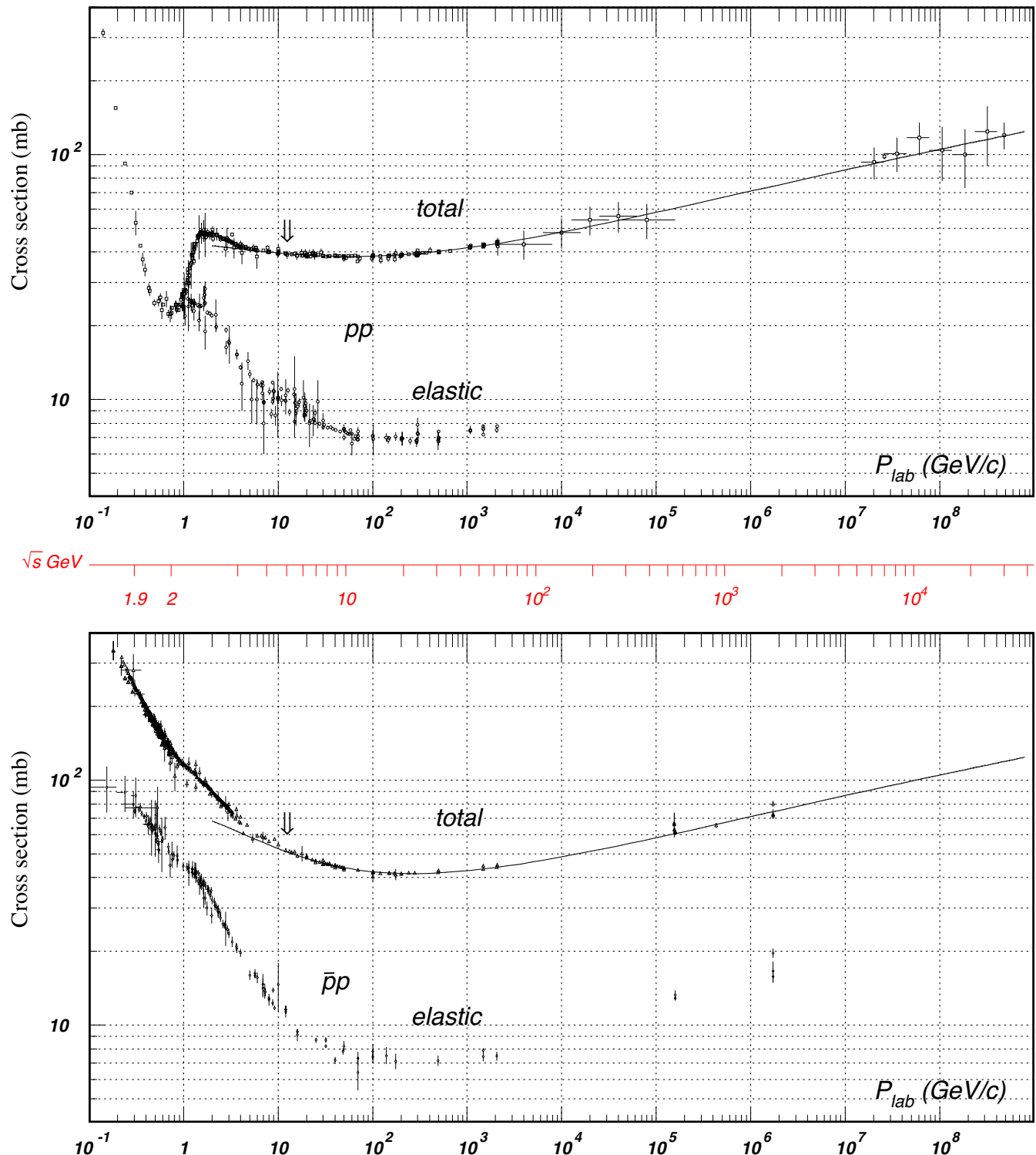


Figure 46.10: Total and elastic cross sections for pp and $\bar{p}p$ collisions as a function of laboratory beam momentum and total center-of-mass energy. Corresponding computer-readable data files may be found at <http://pdg.lbl.gov/current/xsect/>. (Courtesy of the COMPAS group, IHEP, Protvino, April 2012)

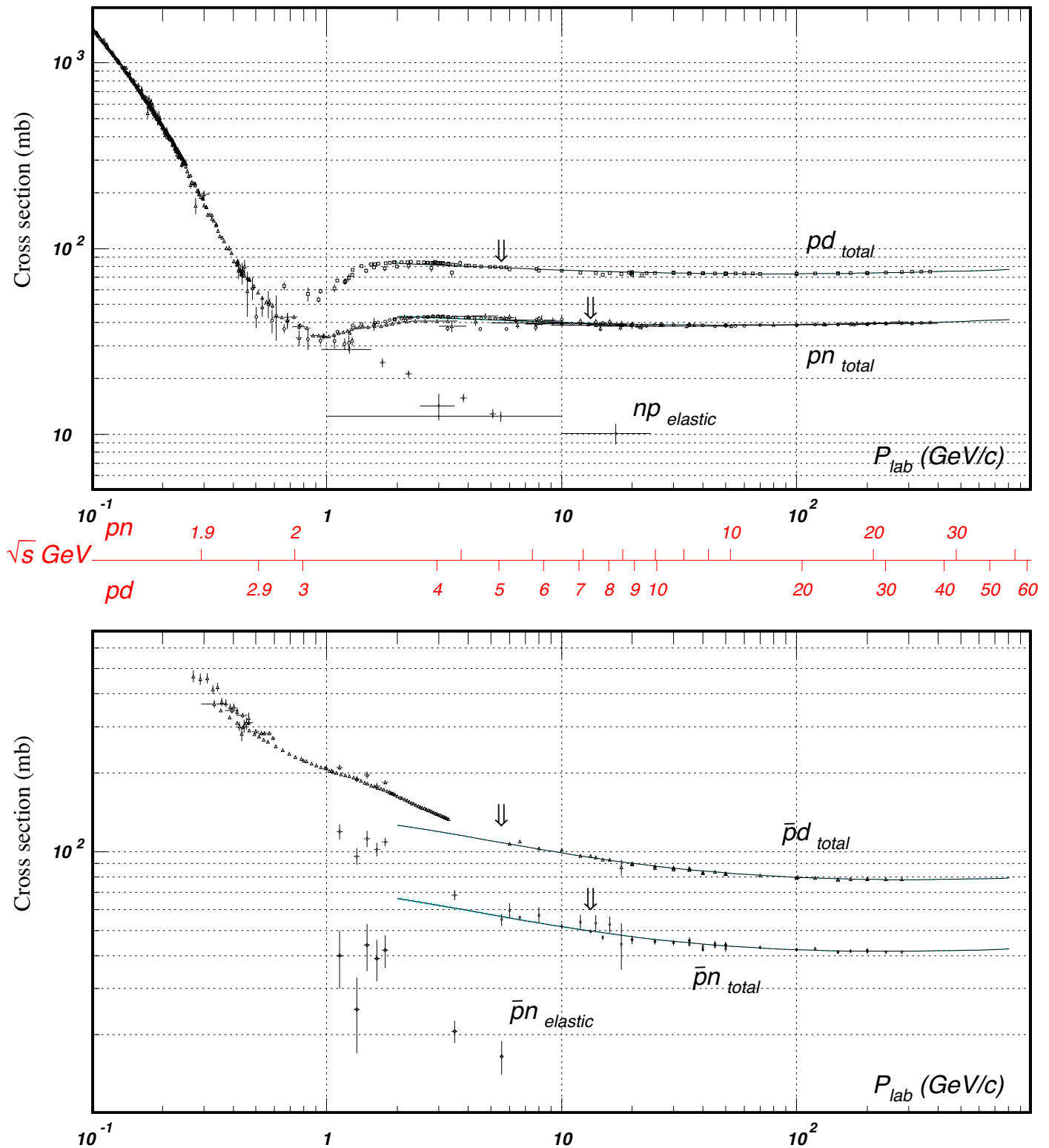


Figure 46.11: Total and elastic cross sections for $p\bar{d}$ (total only), $n\bar{p}$, $\bar{p}d$ (total only), and $\bar{p}n$ collisions as a function of laboratory beam momentum and total center-of-mass energy. Corresponding computer-readable data files may be found at <http://pdg.lbl.gov/current/xsect/>. (Courtesy of the COMPAS Group, IHEP, Protvino, April 2012)

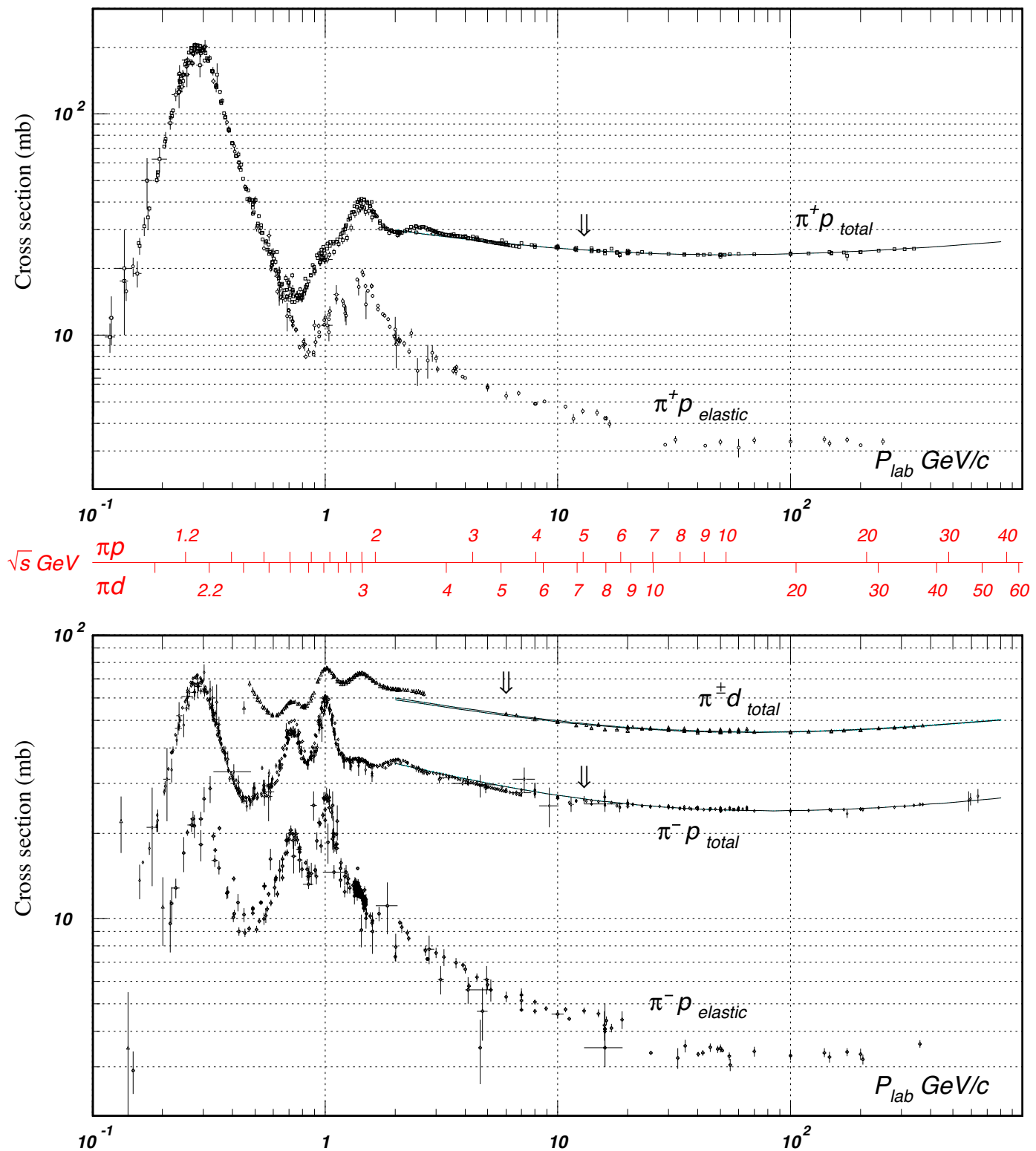


Figure 46.12: Total and elastic cross sections for $\pi^\pm p$ and $\pi^\pm d$ (total only) collisions as a function of laboratory beam momentum and total center-of-mass energy. Corresponding computer-readable data files may be found at <http://pdg.lbl.gov/current/xsect/>. (Courtesy of the COMPAS Group, IHEP, Protvino, April 2012)

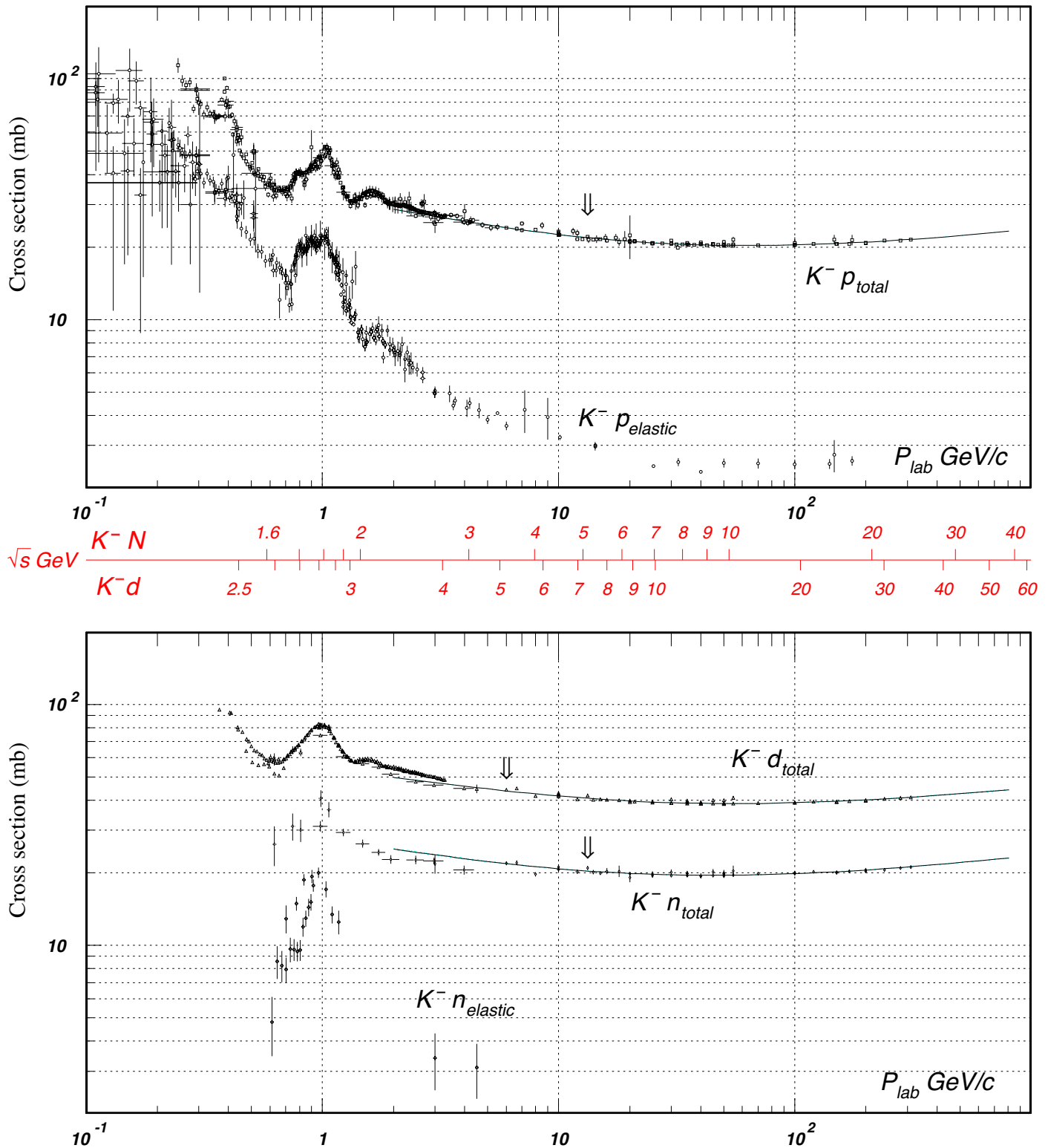


Figure 46.13: Total and elastic cross sections for $K^- p$ and $K^- d$ (total only), and $K^- n$ collisions as a function of laboratory beam momentum and total center-of-mass energy. Corresponding computer-readable data files may be found at <http://pdg.lbl.gov/current/xsect/>. (Courtesy of the COMPAS Group, IHEP, Protvino, April 2012)

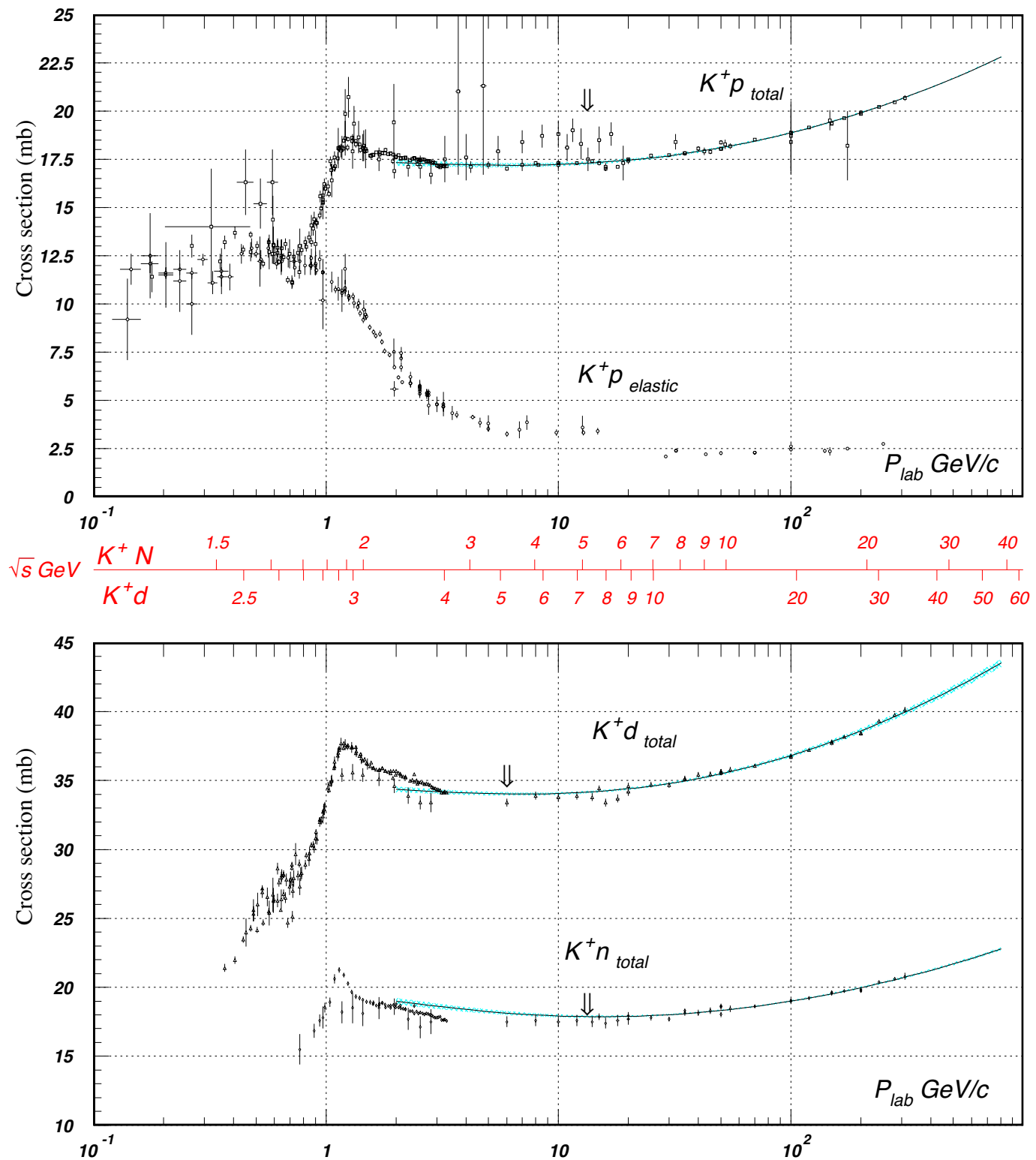


Figure 46.14: Total and elastic cross sections for $K^+ p$ and total cross sections for $K^+ d$ and $K^+ n$ collisions as a function of laboratory beam momentum and total center-of-mass energy. Corresponding computer-readable data files may be found at <http://pdg.lbl.gov/current/xsect/>. (Courtesy of the COMPAS Group, IHEP, Protvino, April 2012)

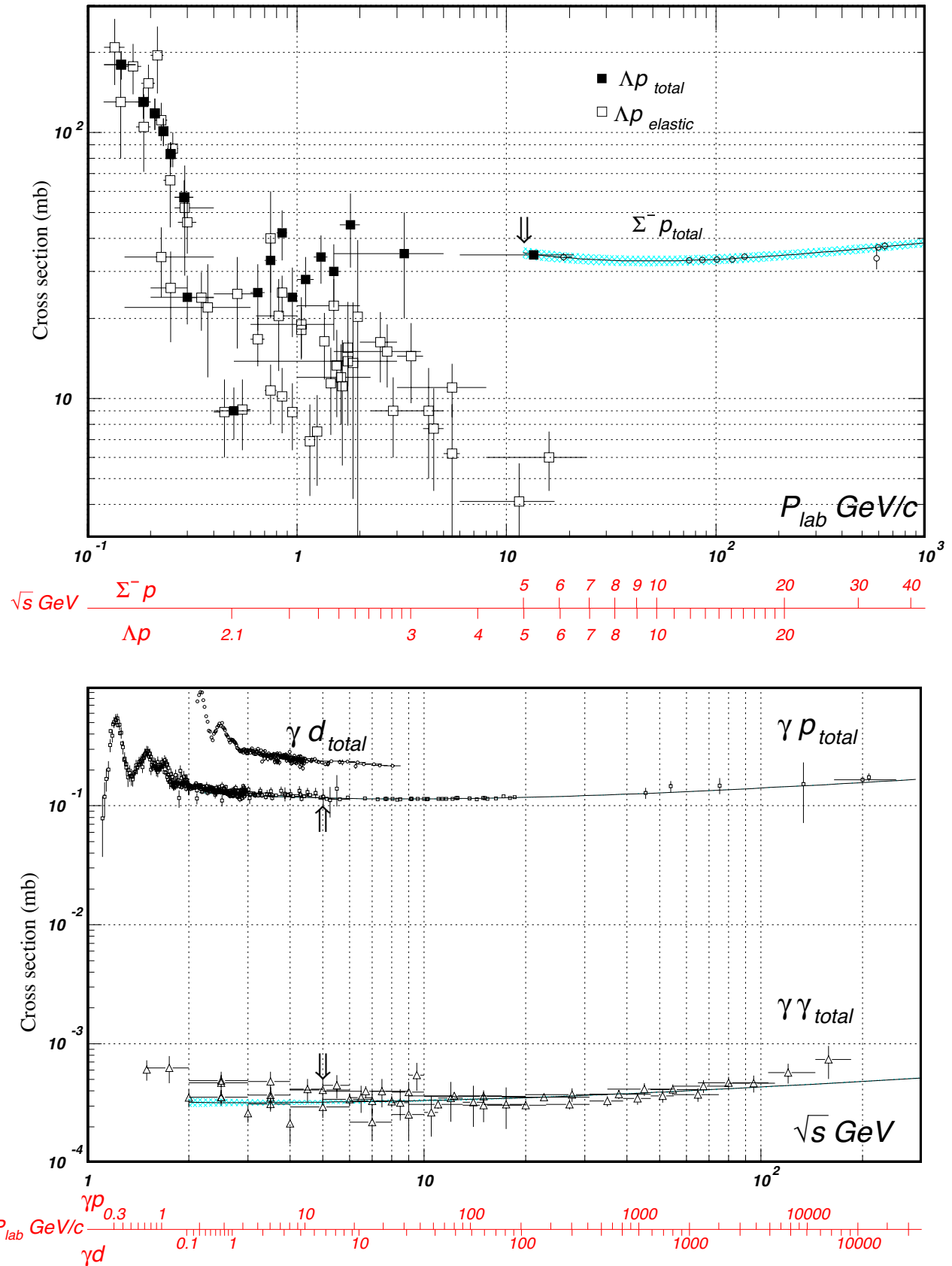


Figure 46.15: Total and elastic cross sections for Λp , total cross section for $\Sigma^- p$, and total hadronic cross sections for γd , γp , and $\gamma\gamma$ collisions as a function of laboratory beam momentum and the total center-of-mass energy. Corresponding computer-readable data files may be found at <http://pdg.lbl.gov/current/xsect/>. (Courtesy of the COMPAS group, IHEP, Protvino, April 2012)